Evaluation of a Passive Millimeter Wave (PMMW) imager for wire detection in degraded visual conditions

Roger Appleby, Peter Coward[*] and John N. Sanders-Reed [†]

ABSTRACT

Ground vehicle tests have been performed to evaluate the performance of a Passive Millimeter Wave (PMMW) imager in reduced visibility conditions and in particular, the ability to detect power lines and cables. A PMMW imager was compared with Long Wave Infrared (LWIR) and visible imaging cameras. The three sensors were mounted on a Land Rover, together with GPS and digital recording system. All three sensors plus the GPS data were recorded simultaneously in order to provide direct comparisons. The vehicle collected imagery from a number of sites in the vicinity of Malvern, UK, in January, 2008. Imagery was collected both while the vehicle was stationary at specific sites and while it was moving. Weather conditions during the data collection included clear, drizzle, rain and fog. Imagery was collected during the day, at night, and during dusk/dawn transition periods. The PMMW imager was a prototype which operated at 94 GHz and was based on a conically scanned folded Schmidt camera and the LWIR and visible sensors were commercial off the shelf items.

Keywords: Millimeter Wave, imaging, wire detection, degraded visual conditions, brown-out, Passive millimeter wave

1. INTRODUCTION

The detection of overhead power cables by rotary wing pilots is essential for safe operation of helicopters. Pilots identify wires and pylons on maps during route planning and keep a lookout for these features during take-off, landing and low level transit. Problems arise when either the map quality is poor or the visibility is reduced. Poor map quality can be augmented by real time aerial reconnaissance data which can be obtained in a more timely manner in a military scenario. Reduced visibility can occur as a result of several factors including low light level, atmospheric obscuration and low contrast of the wire to its background.

The problem of reduced visibility can be overcome by the use of other sensors which either amplify the available light or operate in a different waveband. Night vision goggles (NVG's) which amplify the ambient light can be used at dawn, dusk and at night as long as the ambient light level is sufficient. However all colour information is lost and NVG's are affected badly by bright light sources in the field of view and cannot penetrate obscurants such as smoke, cloud, fog and dust. The contrast mechanism is also similar to that observed in daylight but can vary as the optical properties of the background can differ. Thermal imaging (3-5μm or 8-14 μm) with its increased wavelength can penetrate atmospheric obscurants more effectively but performance is limited in cloud, fog, dust and snow. Millimeter wave imaging (3mm) has a wavelength which is approximately 1000 times longer than that used in thermal imaging and is capable of penetrating atmospheric obscurants that thermal imaging cannot.

Infrared systems have previously been used to observe overhead wires. The initial interest was for maintenance on high voltage national grid cables[1] with the recognition that the insulators that are used to support the cable will heat up if they start to break down. Infrared systems have also been used for pilotage at night and can see cables at distance. Millimeter wave collision avoidance radar has been considered for detecting power cables[2] with the angular dependence of the reflected signal proving particularly challenging. Polarimetric techniques have been applied to overcome this difficulty and further improve detection. The radar cross section of cables has also been extensively modeled[3] and is leading to new detection algorithms.

[*] QinetiQ, Malvern, Worcester, WR14 3PS, UK
[†] Boeing-SVS, Inc. 4411 The 25 Way NE, Albuquerque, NM 87109, USA

In this paper we study the benefits of using multispectral imagery for wire detection by comparing and contrasting data collected in the visible, infrared and millimeter wave spectrum. In section 2 the specification of each sensor is given along with the contrast mechanism in each waveband. In section 3 the results from a data collection trail are presented and analysed. In section 4 we examine potential improvements in the millimeter wave sensor as the unit used in the data collection was an early prototype and finally a summary is given in section 5.

2. SIGNATURES AND SENSORS

2.1. Data Collection

To evaluate the performance of sensors on a moving platform against overhead cables a trials vehicle was fitted out as shown in Figure 1. The infrared and visible sensors are mounted inside a weather proof enclosure which is located just below the passive millimeter wave (PMMW) imager which is enclosed inside a polythene radome. The data from all three sensors and a GPS were recorded digitally using Streams 5[4] software running on a PC.

The specification for each sensor is given in Table 1. When comparing sensors from different wavebands with different imaging mechanisms it is important to consider the meaning of the different parameters. The Instantaneous Field of View (IFOV) is used in the visible and infrared to describe the angle subtended by the detector which can often be larger than the Point Spread Function (PSF) and limit the spatial resolution. In the passive millimeter wave sensor IFOV has no meaning as the PSF is sampled using a horn. Beamwidth is often used in passive millimeter wave and is identical to PSF. A pixel is defined as a picture point at the display.

Figure 1 Trails vehicle with sensors fitted

Parameter	Xybion ISG-750	Merlin	PMMW
HFOV (deg)	27	40	54
VFOV(Deg)	17	30	27
H Pixels	756	320	544
V Pixels	484	240	314
IFOV(mrad)	0.6	2.2	-
PSF[FWHH] (mrad)	0.1	0.7	7.8
Aperture (mm)	13.9	17.9	500
Focal length (mm)	25	25	300
F No.	1.8	1.4	0.6
Output bits	8	12	16
Wavelength (µm)	0.4 -0.9	7-14	3000- 3750
Sensitivity	1800µA/Lm	~100mK	1K

Table 1 Specifications of imaging systems

2.1.1. Sensors

A visible band Low Light Level TV (LLLTV) the Xybion[5] model ISG-750 which uses an image intensified video camera to facilitate operation at reduced levels was used. It operated from 0.4 to 0.9 µm and had a beamwidth of 0.1 mrad. For daylight operation it was fitted with a neutral density filter to prevent saturation of the image intensifier. The long wave infrared (LWIR) sensor was a microbolometer Merlin imager from Indigo Systems[6]. It operates from 7-14 µm and had a beamwidth of 0.7 mrad. The PMMW[7] was a prototype operating at 94 GHz. It used a Schmidt-Cassegrain antenna folded using polarization and is shown in Figure 2 mounted on its gimbals. It has a 500 mm aperture which is defined by the rotating scanner which can also be seen in the figure. Linear polarized light enters from the right passing through the front polarizing mirror and the quarter wave plate. On exit from the quarter wave plate the light is circularly polarized and then is reflected from the scanner which consists of a mirror sandwiched in a foam cylinder. The light then passes back through the quarter wave plate and arrives at the front polarizing mirror orthogonally polarized to the input and is focused down onto a receiver array consisting of 5 rows of 30 receivers. This antenna system results in an image of the scene being scanned across the receiver array in a circular motion. This imager operates from 3 to 3.7 mm (80-100 GHz) and has a beamwidth of 7.8 mrad.

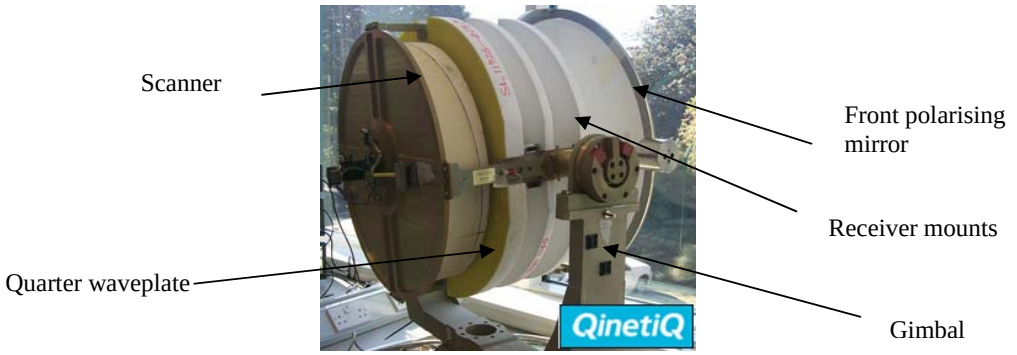

Figure 2 PMMW sensor

2.2. Cable Signature

The overhead cables available for this work consisted of helical aluminium rods approximately 3mm in diameter on a steel former as shown in Figure 4. The cables were ~14.5 mm and were supported on steel pylons. There are many different forms of cable construction[8] and it is impossible to be certain of the exact form in this case as the cables were in use and could not be examined.

The ability to detect a cable is determined by the contrast C_c of the cable to its background as shown in equation 1

$$Cc = \frac{L_B - L_c}{L_B + L_c} \qquad 1$$

where L_B is radiance of the background and L_c is the radiance of the cable. Radiance is the sum of both the reflected and emitted radiation. It should also be noted that in the visible region radiance is referred to as luminance. The contrast detected by the sensor is a function of the point spread function θ and is given in equation 2 at the full width at half height (FWHH)

$$\theta = \frac{1.22\lambda}{d} \qquad 2$$

where λ is the wavelength and d the aperture diameter. This is often referred to as the beamwidth in the MMW region. Figure 3 shows two beams, one with the cable and one with background. Cables are typically detected at long range were the beamwidth is considerably wider than the diameter of the cable. The radiance of the beam imaging the cable will therefore be reduced by the fill factor F which is given in equation 3.

$$L_{CF} = L_B(1-F) + L_C F \qquad 3$$

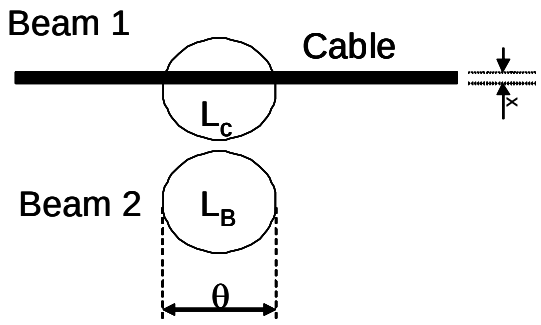

Figure 3 Beam Fill

Figure 4 Examples of overhead cables, top 12mm diameter as manufactured, bottom 8mm diameter after weathering

F is the fraction of the beam occupied by the cable with a diameter of x at a range R and is given in equation 4. It is assumed that the cable passes through the centre of the beam. When the IFOV is greater than θ *it* limits the spatial resolution and should be substituted into equation 4. Table 1shows this is the case for the LWIR and LLTV.

$$F = \frac{4x}{\theta R \pi} \qquad 4$$

In the infrared the radiance of an object is related to its temperature through the Stefan-Boltzman Law[9] and in the millimeter wave region the radiance of an object is directly proportional to its temperature as stated by the Rayleigh Jeans Law[10].

2.2.1. Atmospheric Propagation

The contrast of the cable C_c is further reduced by atmospheric propagation. In general for horizontal viewing through the atmosphere we must consider two loss mechanisms. The first is due to scattering or absorption which reduces the amount of light reaching the observer and the second is due to light scattered into the viewing path from all other sources of light – the sun, the sky, clouds and ground[11]. The radiance of a cable $L_c(R)$ at range R is given by equation 5 where the first term is due to scattering or absorption and the second term is due to light scattered into the viewing path and here L_B is the background radiance and α is the extinction coefficient.

$$L_c(R) = L_C e^{-\alpha R} + L_B\left(1 - e^{-\alpha R}\right) \qquad 5$$

In the visible spectrum the contrast at range R is often modeled by the Koschmeider's equation[11] which is a simple theory developed for viewing through a controlled atmosphere.

The attenuation in the atmosphere has recently been modeled across the millimeter wave, infrared and visible regions[12]. The values for a standard atmosphere 7.5g/m^3 of water vapour, T=20 C, P=1013 Pa, a fog with 100 m visibility and rain at 4 mm/hr are given in Table 2. The data in the table shows that attenuation falls off as wavelength increases.

Visibility is defined as being the distance to an object where the image contrast drops to 0.02 of what it would be if the object were nearby. It is usually measured with a black object against a white background and is quoted at 550 nm. The values for fog in the visible in Table 2 are incorrect as the contrast should fall to 0.02 when calculated using equations 1 and 5 but it only falls to 0.24. Attenuation Γ has been estimated from visibility V as shown in equation 6 which was developed by Kruse for fog and cloud[13]

$$\Gamma(V,\lambda) = \frac{K}{V} \qquad 6$$

where K> 8.5 and K <17 db. Using a value of 12 db, which from ref.16 would include light being scattered into the observers field of view gives an attenuation of 120 db which equates to a contrast of 0.02 and a value of 120 db is shown in square brackets in the table. In an experimental comparison of fog attenuation in the visible and infrared Colvero et al[14] also found an attenuation of 120 dB in the visible for 100m visibility and an associated attenuation at 10 μm of 27 dB and this value is also shown in square brackets in the table.

	Attenuation db/km		
Spectral Region	**STD**	**Rain (4 mm/hr)**	**Fog (Visibility 100 m)**
Visible (0.4 -0.9 μm)	2	2	35 [120]
Infrared (7-14 μm)	0.4	0.4	10 [27]
Millimeter Wave (3-3.75 mm)	0.4	3.2	0.4

Table 2 Atmospheric Attenuation [Values in brackets calculated according to Refs. 14 and 15]

The values in square brackets were used in the contrast predictions shown in Table 3.

2.2.2. Visible sensor

The contrast in this waveband is generated from reflected light. The surface of the aluminum cable is weathered with a thin layer of black material which is most likely carbon and is black in this waveband as shown in Figure 4. The figure

also shows that in some cases between the strands bare aluminium can be seen. The cable appears darker than the background in most of the imagery but in one section it appears light which in this case is attributed to sun glint. It is difficult to estimate the reflectivity of the cable but it is likely to have a low reflectivity and a value of 0.1 was used. The PSF of 0.1 mrad results in a beamwidth of 10 mm at 100m and 50mm at 500m. The spatial resolution is however limited by the IFOV to 0.6 mrad.

2.2.3. Infrared Sensor

The contrast in this waveband is generated from emitted light. The cable appears warm against its background in the imagery and it is likely that the contrast in this waveband is generated mostly from emission from the weathering. The temperature of an overhead cable is a function of the ambient conditions and the electrical load[15]. The distribution company[16] estimated the temperature is typically 10 C above ambient. The apparent radiometric temperature will be modified according to the Steffan Boltman law but here we will use the physical temperature. A reflectivity of ~0.1 was used. The PSF of 0.7 mrad results in a beamwidth of 70 mm at 100m and 320mm at 500m. The spatial resolution is however limited by the IFOV to 2.2 mrad.

2.2.4. Passive Millimetre Sensor

The contrast in this waveband is generated by reflection from the underlying aluminium. The cable appears cold against the background in the image. The black layer produced by weathering seems to be transparent and so the top half of the cable will reflect the sky which can be as cold as 50K in this waveband and the bottom half will reflect the ground which will be at approximately 300 K. This will result in the cable appearing colder than the background in the image. A reflectivity of 1 is assumed. The PSF of 7.8 mrad results in a beamwidth of 780 mm at 100 m and 3900 mm at 500 m.

2.2.5. Theoretical Sensor Performance

Using equations 1-5 we can estimate the contrast of a 14.5 mm wire at 100 m in each waveband as shown in Table 3. This estimate is for the contrast at the entrance to the camera and not as displayed to the observer. This was done for clear air and also for fog where the visibility is 100 m. It was assumed that L_B the background radiance is equal to the radiance produced by the ambient conditions and that the atmosphere is homogeneous. In the visible spectrum the radiance of the cable is unknown and the contrast is estimated from the reflectivity.

Parameter	**Visible (Xybion ISG-750)**	**LWIR (Merlin)**	**PMMW**
Fill factor (F)	0.3	0.08	0.01
Background radiance L_B	-	283	283
Estimated Cable Reflectivity	0.1	0.1	1
Cable radiance L_c	-	293	50
Cable radiance modified by Fill Factor L_{cF}	-	286	280
Contrast C_c	0.8	-0.02	0.7
Contrast $C_c(100)$ Clear day	0.15	-0.001	0.005
ΔT K *(100)* Clear day		0.8	2.6
Contrast $C_c(100)$ fog	0.009	-0.0008	0.005
ΔT K *(100)* fog		0.45	2.6

Table 3 Theoretical contrast of a 14.5mm cable at a range of 100m

C_c in the visible is 0.8 and is reduced to 0.15 at 100m in clear air by a combinations of a fill factor of 0.3 and atmospheric loss. In fog the contrast is reduced to 0.009 and the cable would not be seen by eye. In the infrared C_c is -0.02 as the cable radiance is higher than the background. It is reduced at 100m both by the fill factor 0.08 and attenuation to -0.001. The clear air attenuation (0.4db/km) is however lower than the visible (2db/km). In fog the cable will still be visible but the contrast is reduced to -0.0008 but would still be visible as this is above the detection limit of the camera. In the millimeter wave region C_c is high at 0.7 but is reduced to 0.005 at 100m in clear air by the fill factor with the attenuation having virtually no effect. In fog the contrast remains the same as the attenuation has no effect. In clear air and fog the

temperature difference from the cable at 100 m at the entrance to the camera is greater than the sensitivity for both the LWIR and PMMW cameras and the cable will be seen.

3. RESULTS AND ANALYSIS

The primary data collection was carried out in January 2008 on a roads located near Malvern UK at approximately 52° 03' 59.18" N and 2° 17' 15.67" W. The road at this location passes under a power line suspended from pylons and passes over a hill when travelling west to east. Travel in a westerly direction provides a view of the cables against the ground as shown in Figure 5 and in an easterly direction a view of the cable against the sky as shown in Figure 6. Data was collected over a two week period for both day and night and in several different weather conditions ranging from clear to overcast and on one occasion there was fog. The zenith sky temperature in the millimeter wave band was monitored and varied from 50K on clear days to >200K on overcast days.

A still image extracted from one of the video sequences is shown in Figure 5 and illustrates the performance of the different sensors with a terrain background with cables. The range to the cables here is 160m. It should be noted that objects are more visible when viewed in the video sequences than in the still imagery due to the motion and changes in perspective. This data was collected on a clear sunny day and illustrates the different phenomenology in each waveband. The PMMW on the left has high contrast but relatively low resolution and is dominated by reflectivity, the LLTV in the centre has high resolution and is dominated by reflection and the LWIR on the right has intermediate resolution and is dominated by emission. The pylon is visible in all three images having a positive contrast in the millimeter wave and LWIR image and a negative contrast in the visible. The cable will have a similar contrast in each case and is at the limit of detection in the millimeter wave image at 160m. This figure illustrates the difficulty of detecting cables in different wavebands and shows how contrast is strongly influenced by the background and associated clutter in the different wavebands.

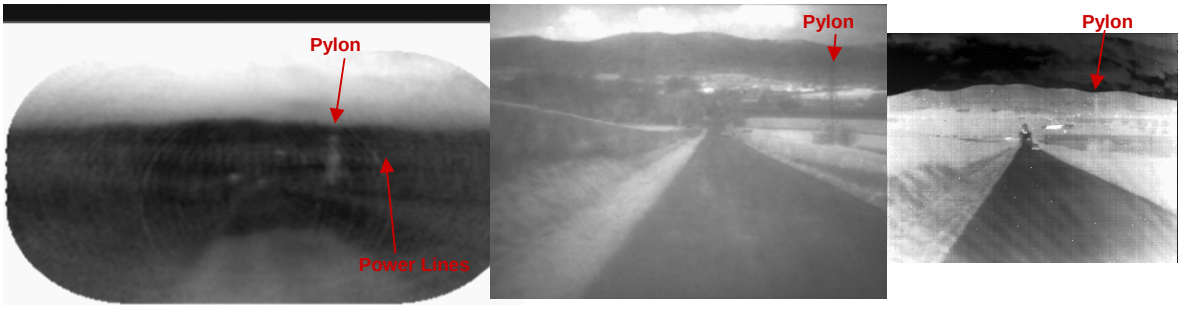

Figure 5 Left PMMW, middle LLLTV, right LWIR imagery in look down geometry.

Data collected at night gave similar performance in the PMMW and LWIR images. Data collected in degraded visual environments gave results for the PMMW sensor which were worse than predicted and this is discussed further in section 4.

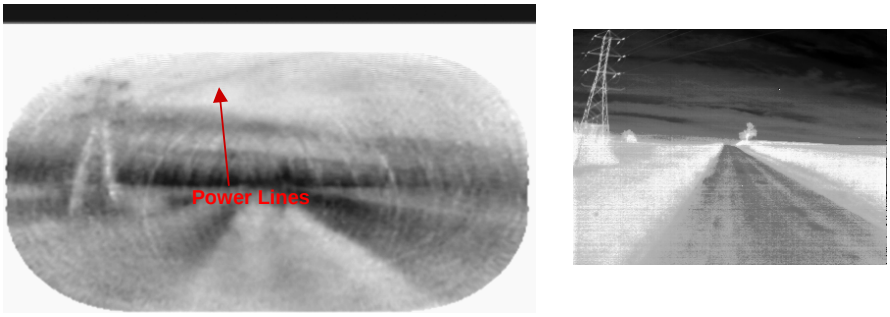

Figure 6 Left PMMW, right LWIR imagery look up geometry at night

Figure 6 shows data collected at night and here the cables at a range of 20m have a sky background.

Table 3 indicates that the PMMW should be able to detect the cable at around 100m which was achieved in the data collection.

In this data the PMMW sensor outperforms the LLLTV and LWIR imagers in many respects for power line imaging. However improvements could be made to the LWIR and LLTV to improve the fill factor by increasing the focal length of the lens on the camera and keeping the F number constant. This would reduce the field of view but increase the spatial resolution and improve the fill factor. This would also be possible in the PMMW imager but would require a large increase in the size of the camera which would not be commensurate with most applications.

4. SENSOR ENHANCEMENTS

The PMMW sensor used is a prototype device and as seen from Figure 5 and Figure 6 some circular artifacts are visible in the image. These artifacts are generated by variability in the receivers. This in principle is corrected by image processing but when the difference between receivers is too great circles appear in the image. This imager uses direct detection receivers based on three MMIC chips fabricated at Hughes Research Laboratories[17] (HRL) and a hybrid detector[7]. HRL have recently introduced the LNA5-100 and V1A MMICs which reduces the RF component count from four to two. This new chipset, which we have tested in prototype receivers, will improve the sensitivity by a factor of 2 and should considerably reduce the variation between receivers.

Since these trials the optical performance of the sensor has been investigated in some detail and the PSF of the system used was found to be worse than the theory predicted. Whilst the central peak was approximately the right width, its height was reduced and the sidelobes were greater than anticipated. The PSF was improved by setting up the optics on an optical bench in the laboratory rather than in the framework used for these trials and a result very similar to the calculated PSF was obtained. It is estimated that during this work approximately 66% of the radiation leaked out of the main beam and appeared in sidelobes. The result of this leakage would have been to reduce the contrast and apparent sharpness of the image due to the energy in sidelobes contributing to adjacent pixels.

A second generation imager has been designed and is in the process of being manufactured. This imager will use the new HRL chipset and be designed to ensure good optical performance.

5. SUMMARY

Simultaneous visible (LLLTV), LWIR, and PMMW imagery of power lines against sky and terrain backgrounds during day and night, clear weather, rain, and some fog was collected. PMMW has a much lower resolution than the other sensors and is approximately four times less than LWIR and thirteen times less than the visible. Nevertheless, the PMMW imager was able to image power lines at a range of 160m. Further improvements to the imager could increase this by a factor of three.

It was also surprising that in clear conditions, the PMMW was able to image power lines when the LWIR and LLLTV could not, despite their much higher resolution which indicates that the PMMW contrast must be higher. While the PMMW out performed the LLLTV and LWIR imagers in many respects for power line imaging, it must be understood that the the LLLTV and LWIR can be significantly improved by changing the lens.

ACKNOWLEDGEMENTS

The authors wish to acknowledge the support of the UK MoD and Boeing for funding the work on this project.

REFERENCES

[1] Provost, D., “Infrared thermography at EDF : a common technique for high-voltage lines but new in monitoring and diagnosis of PWR plant components”, Proc. SPIE 2766, 83-90, (1996).

[2] Rembold, B., Wippich, H. G., Bischoff, M. and Frank, W. F. X., “A MM-wave collision warning sensor for helicopters, Proc. Military Microwave”, 344–351, (1982).
[3] Sarabandi,K. and Park, M., A Radar Cross-Section Model for Power Lines at Millimeter-Wave Frequencies, IEEE Trans. on Ant. and Prop., 51(9), 2353-2360, (2003).
[4] http://www.ioindustries.com/
[5] http//:www.xybioncameras.com
[6] http://www.indigosystems.com
[7] Appleby R., Anderton R. N., Price S., Salmon N. A., Sinclair G. N., Coward P. R., Barnes A.R., Munday P. D., Moore M., Lettington A. H. and Robertson, D.A., “Mechanically scanned real time passive millimetre wave imaging at 94GHz”, Proc. SPIE 5077, (2003)
[8] http://aluminium.matter.org.uk/content/html/ENG/default.asp?catid=164&pageid=2144416510
[9] Lloyd,J.M. [Thermal Imaging Systems], Plenum Press, (1975).
[10] Kraus,J.D. [Radio Astronomy], Cygnus-Quasar, (1986).
[11] Overington,I., [Vision and Acquisition], Pentech Press, (1976).
[12] Appleby,R. and Wallace,H.B., Standoff detection of weapons and contraband in the 100 GHz to 1 THz region, IEEE Trans Ant and Prop., 55(11), 2944-2956, (2007).
[13] Fischer,K.W., Witiw,M.R. and Eisenberg,E. “Optical attenuation in fog at a wavelength of 1.55 micrometers, Atmospheric Research”, 252-258, (2008).
[14] Colvero,C.P., Cordeiro,M.C.R., de Faria,G.V. and von der Weid, J.P., “Experimental comparison between far- and near infrared wavelengths in free space optical systems”, Microwave and Optical technology Letters, 46, 319-322, (2005).
[15] Bockarjova,M., and Andersson,G., “Transmission Line Conductor Temperature Impact on State Estimation Accuracy”, Power Tech 2007 IEEE Lausanne, 701-706, (2007).
[16] Central Networks private communication, http://www.eon-uk.com/distribution/
[17] http://www.hrl.com/media/hemt/hemt_cmrcl.html